

On the Double-Generalized Gamma Statistics and Their Application to the Performance Analysis of V2V Communications

Petros S. Bithas, *Member, IEEE*, Athanasios G. Kanatas, *Senior Member, IEEE*, Daniel B. da Costa, *Senior Member, IEEE*, Prabhat K. Upadhyay, *Senior Member, IEEE*, and Ugo S. Dias

Abstract—Important statistical properties of the double-generalized Gamma (dGG) distribution are studied in this paper. The dGG distribution is suitable for modelling non-homogeneous double-scattering radio propagation fading conditions, which can be frequently observed in vehicle-to-vehicle (V2V) communications. In this context, important statistical metrics for the bivariate dGG distribution, such as the joint probability density function, cumulative distribution function, and the moments, are derived for the first time, while simplified expressions for the corresponding marginal statistical metrics are presented. Moreover, the second-order statistics of this distribution are also analytically studied. The derived analytical framework has been employed to analyze the performance of a transmit antenna selection system operating in V2V communication channels modeled by the dGG distribution. In this scenario, the impact of outdated channel state information (CSI) to the system's performance is investigated in terms of various metrics including the level crossing rate and the average fade duration. Furthermore, simplified asymptotic closed-form expressions for the outage probability have been derived to examine the achievable diversity and coding gains. Based on our analysis, insightful discussions are provided. It is shown that the diversity gain is independent from the number of transmit antennas when the available CSI becomes outdated.

Index Terms—Average fade duration, correlated statistics, double-generalized Gamma, level crossing rates, outdated channel estimates, transmit antenna selection, V2V communications.

I. INTRODUCTION

With the rapid growth of information and communication technologies (ICTs), intelligent vehicles, using the on-board units and the wireless communications capabilities,

Manuscript received XXX XX, 2017; revised XXXXXXX X, 2017; accepted XXXXXXX X, 2017. Date of publication XXXXXX XX, 2017; date of current version XXXXX XX, 2017. This research has received funding from the European Union's Horizon 2020 research and innovation programme under "ROADART" Grant Agreement No 636565.

P. S. Bithas and A. G. Kanatas are with the Department of Digital Systems, University of Piraeus, 18534 Piraeus, Greece (e-mail: {pbithas, kanatas}@unipi.gr).

D. B. da Costa is with the Department of Computer Engineering, Federal University of Ceará (UFC), Sobral-CE, Brazil (e-mail: danielb-costa@ieee.org). The work of Prof. D. B. da Costa was supported by the CNPq (Grant No. 304301/2014-0).

P. K. Upadhyay is with the Discipline of Electrical Engineering, Indian Institute of Technology Indore, Madhya Pradesh, India (e-mail: pkupadhyay@iiti.ac.in). The research work of P. K. Upadhyay was supported in part by the Young Faculty Research Fellowship of MeitY, Govt. of India.

U. S. Dias is with the Department of Electrical Engineering, University of Brasília, DF, Brazil (e-mail: ugodias@ieee.org). The work of U. S. Dias was partially supported by the Ministry of Justice, Govt. of Brazil, under grant TED-FUB-SENACON/MJ 001/2015.

Digital Object Identifier 10.1109/TCOMM.2017.2710196

will be considered as mobile resources, revolutionizing thus the automotive sector. The idea behind this integration is that the connected vehicles can cooperatively exchange information, based on coordinated or distributed approaches. The driving forces for this integration is to support various applications for road safety, smart and green transportation, location dependent services, and in-vehicle Internet access [1]. However, comparing the characteristics of the traditional (cellular) networks to the corresponding ones of vehicular ad-hoc networks (VANETs), the following major differences may be highlighted: i) the channel behavior is highly time varying, given the fact that VANETs are characterized by higher mobility as compared to the cellular ones, ii) low complexity requirements dominating the transceiving systems, since many signal processing, hardware, and space limitation constraints arise, when trying to integrate these systems in vehicles, and iii) both the transmitter and the receiver are in motion, while they are in the same height, resulting to channel models with unique characteristics.

In mobile-to-mobile (M2M) communications, waves are supposed to be scattered and re-scattered around both the transmitter's and the receiver's local environments. This double-bouncing procedure has been modeled as a product of fading amplitudes [2]. Widely adopted distributions for modeling the double-bouncing scattering are the double-Rayleigh (dR), double-Nakagami (dN), and double-Weibull (dW) [3]–[5]. In addition, these models offer good fit to experimental data for M2M communications, as it is verified by many experimental channel measurement campaigns, e.g., [6]. Their excellent physical justification and their agreement with empirical results explain why these distributions have been adopted by many authors for modeling M2M communication environments, e.g., [7]–[10]. Specifically, in [7] and [8], the level crossing rate (LCR) and average fade duration (AFD) of dN fading process has been studied. In [9] and in [10], the performance in terms of bit error probability of diversity schemes in dR and dN channels, respectively, was studied. Nevertheless, all aforementioned double-bouncing distributions represent special cases of the double-generalized Gamma (dGG), which can accurately model a plethora of different mobile propagation conditions.

The dGG random variable (RV) is defined as the product of two α - μ (generalized-Gamma (GG)) RVs and thus it can efficiently explore the nonlinearities of the propagation medium, which frequently appear in non-homogeneous environments.

The dGG distribution, includes important distributions such as Gamma-Gamma, dN, dW, Weibull-Gamma, and dR, while it can also efficiently describe the Nakagami/Rayleigh-lognormal as well as GG as limiting cases. Moreover, it is mathematically tractable, in the sense that easy-to-compute closed-form expressions can be obtained, which provide useful insights to the system's performance. Thus, its generic nature can effectively be exploited to model all different fading conditions in environments that change very fast, as the ones appearing in vehicle-to-vehicle (V2V) communication scenarios. Recently, in [11], [12], the dGG distribution has been employed to model the turbulence-induced fading in free-space optical communication systems, in which the first order statistics have been studied. In the context of wireless communications, many efforts have been devoted to analytically describe important statistical metrics of this distribution, which, in general, have led to approximated solutions, e.g., [13], [14]. Nevertheless, important statistical characteristics of this generic distribution have not been thoroughly studied yet. Such an analytical framework can be used to investigate the performance of emerging and future wireless communication systems and this is the subject of the current paper.

As far as low complexity communication systems are concerned, transmit antenna selection (TAS) has been considered as a quite attractive approach, e.g., [15], [16]. Based on this technique, a single transmit antenna from a set of L available ones, which maximizes the total received signal power at the receiver, is selected for transmission. Recently, in order to reduce the number of expensive radio frequency (RF) chains, this technique has been also employed in the area of inter-vehicular communications, e.g., [17], [18]. It is noteworthy that in previous studies in this area, perfect channel state information (CSI) is assumed to be available at the receiver for the antenna selection procedure. However, due to the high mobility, the wireless medium will be highly time varying, resulting to outdated knowledge of the CSI. Therefore, the ideal CSI assumption has only theoretical importance and cannot be established in practice, especially in VANETs [19], [20]. Thus, to the best of the authors' knowledge, no other work has investigated first and second order statistics of TAS system (with L antennas) in a V2V communication scenario and under the assumption of outdated CSI.

Motivated by the aforesaid observations, the dGG fading distribution is employed for the first time for modeling the V2V communication channels, exploiting thus its versatility to accurately describing this kind of environments. In this context, the contribution of the paper can be summarized as follows:

- Important statistical characteristics for the *bivariate* and *marginal* statistics of the dGG distribution with non-identical parameters are presented;
- The *second-order* statistics of this generic model have been also presented for the first time;
- The signal-to-noise ratio (SNR) statistics of a TAS scheme operating in dGG fading environment is investigated, taking also into consideration the impact of outdated CSI due to the feedback delay;
- The performance of this scheme has been studied in terms of the outage probability (OP), symbol error probability

(SEP), average capacity, LCR, and AFD;

- A high SNR analysis is also provided and employed to identify the coding and diversity gains of the system.

It is noteworthy that the derived results are new and general, while they also encompass many existing ones as special cases.

The remainder of the paper is organized as follows. In Section II, the marginal, bivariate, and second-order statistics of the dGG distribution are presented. In Section III, the system and channel models of the TAS scheme are presented along with a stochastic analysis for the received SNR statistics. In Section IV, the derived analysis is employed for the performance evaluation. In Section V, several representative numerical examples are presented and discussed, while in Section VI, some concluding remarks are provided.

II. DOUBLE GENERALIZED-GAMMA STATISTICS

A. Marginal Statistics

Let $R = G_1 \times G_3$ denote a RV following the dGG distribution, in which G_j ($j \in \{1, 3\}$) are independent GG distributed RVs with probability density function (PDF) given by [21, Eq. (1)]

$$f_{G_j}(x) = \frac{\beta_j m_j^{m_j} x^{\beta_j m_j - 1} \exp\left(-\frac{m_j x^{\beta_j}}{\Omega_j}\right)}{\Omega_j^{m_j} \Gamma(m_j)}. \quad (1)$$

In (1), β_j and m_j are distribution's shaping parameters, $\Omega_j = (\mathbb{E}\langle G_j^2 \rangle \Gamma(m_j) / \Gamma(m_j + 2/\beta_j))^{\frac{\beta_j}{2}} m_j$, $\mathbb{E}\langle \cdot \rangle$ denotes expectation, and $\Gamma(z) = \int_0^\infty e^{-t} t^{z-1} dt$ is the Gamma function [22, Eq. (8.310/1)]. It is noteworthy that the GG distribution includes many distributions, e.g., exponential, Rayleigh, one-sided Gaussian, Nakagami- m , Gamma, and Weibull, whereas it may also describe the lognormal distribution as a limiting case [23]. For example by setting $\beta_j = 1$ in (1), it coincides to the PDF of the Gamma distribution. The GG distribution has been employed for modelling signals composed of clusters of multipath waves propagating in a nonhomogeneous environment [21]. The PDF of R can be obtained by

$$f_R(x) = \int_0^\infty \frac{1}{y} f_{G_1}(y) f_{G_3}\left(\frac{x}{y}\right) dy. \quad (2)$$

For $\beta_3 = \beta_1$, substituting (1) in (2) and applying [22, Eq. (3.471/9)] yield the following expression

$$f_R(x) = \frac{2\beta_1 \hat{\Omega}_1^{\frac{m_1+m_3}{2}}}{\Gamma(m_1) \Gamma(m_3)} \times x^{\frac{\beta_1}{2}(m_1+m_3)-1} K_{m_3-m_1}\left(2\sqrt{\hat{\Omega}_1} x^{\frac{\beta_1}{2}}\right), \quad (3)$$

in which $\hat{\Omega}_1 = m_1 m_3 / (\Omega_1 \Omega_3)$ and $K_v(z) = \frac{\pi}{2} \frac{I_{-v}(z) - I_v(z)}{\sin(v\pi)}$ is the modified Bessel function of the second kind and order v [24, Eq. (9.6.2)], with $I_v(\cdot)$ denoting the modified Bessel function of the first kind [22, Eq. (8.406/1)]. The dGG distribution includes many well-known distributions as special cases, e.g., dR [3], dN [25], and dW [5], [26]. For example, for $\beta_1 = 2$, (3) coincides to the dN PDF, while for $m_1 = m_3 = 1$, (3) coincides to the dW PDF. Therefore, based on its various shaping parameters, the dGG distribution is flexible enough and thus can be efficiently utilized to

provide excellent fit in different V2V channel measurements data, while its mathematical tractability can be exploited for analytical investigations. The corresponding expression for the cumulative distribution function (CDF) of R is given by

$$F_R(x) = \frac{\hat{\Omega}_1^{p_1}}{\Gamma(m_1)\Gamma(m_3)} x^{\beta_1 p_1} \mathcal{G}_{1,3}^{2,1} \left(\hat{\Omega}_1 x^{\beta_1} \middle|_{p_2, -p_2, -p_1}^{1-p_1} \right), \quad (4)$$

with $p_1 = \frac{m_1+m_3}{2}$, $p_2 = \frac{m_3-m_1}{2}$, and $\mathcal{G}_{p,q}^{m,n}[\cdot|\cdot]$ denoting the Meijer G-function [22, Eq. (9.301)]. By setting $\beta_1 = 2$ in (4), it simplifies to [10, Eq. (7)]. It is noted that Meijer G-function is a built-in function in many mathematical software packages, e.g., Mathematica, Maple, and thus can be directly evaluated. An alternative simplified expression for (4) can be extracted as follows. The CDF of R is given by $F_R(x) = \int_0^x \int_0^\infty \frac{1}{y} f_{G_1}(y) f_{G_3} \left(\frac{x}{y} \right) dy dz$. Assuming integer values for m_3 (and arbitrary values for m_1), changing the order of integration, and using first [22, Eqs. (8.350/1) and (8.468)] and then [22, Eqs. (8.310/1) and (3.471/9)], the following mathematically-convenient expression is deduced

$$F_R(x) = \frac{1}{\Gamma(m_3)} \left(1 - \sum_{k_1=0}^{m_3-1} \frac{2\hat{\Omega}_1^{\frac{k_1+m_1}{2}}}{k_1! \Gamma(m_1)} x^{\frac{\beta_1}{2}(k_1+m_1)} \times K_{k_1-m_1} \left(2\hat{\Omega}_1^{1/2} x^{\frac{\beta_1}{2}} \right) \right). \quad (5)$$

Furthermore, for $m_1 = n + 1/2$, with $n \in \mathbb{N}$, employing [22, Eq. (8.468)] and performing some mathematical manipulations yield the following convenient expression for the CDF of R

$$F_R(x) = \frac{1}{\Gamma(m_3)} \left[1 - \sum_{k_1, k_2=0}^{\zeta(m_1, m_3)} D_1 \hat{\Omega}_1^{\frac{k_1+m_1-k_2-\frac{1}{2}}{2}} \times x^{\frac{\beta_1}{2}(k_1+m_1-k_2-\frac{1}{2})} \exp \left(-2\sqrt{\hat{\Omega}_1} x^{\frac{\beta_1}{2}} \right) \right], \quad (6)$$

with $\sum_{k_1, k_2=0}^{\zeta(m_1, m_3)} = \sum_{k_1=0}^{m_3-1} \sum_{k_2=0}^{|k_1-m_1|-1/2}$, $D_1 = \frac{\sqrt{\pi}/2^{2k_2}}{\Gamma(m_1)k_1!k_2!}$, $\frac{(|k_1-m_1|-\frac{1}{2}+k_2)!}{(|k_1-m_1|-\frac{1}{2}-k_2)!}$. Using (3) in [27, Eq. (5.21)] and applying [22, Eq. (6.561/16)], the n_1 th moment of R is given by

$$\mathbb{E} \langle R^{n_1} \rangle = \frac{\hat{\Omega}_1^{-\frac{n_1}{\beta_1}} \Gamma \left(m_1 + \frac{n_1}{\beta_1} \right) \Gamma \left(m_3 + \frac{n_1}{\beta_1} \right)}{\Gamma(m_1)\Gamma(m_3)}. \quad (7)$$

B. Bivariate Statistics

Let R_1, R_2 denote two dGG RVs defined as

$$\begin{aligned} R_1 &= G_1 \times G_3 \\ \rho_G \downarrow \quad \rho_1 \downarrow \quad \rho_2 \downarrow \\ R_2 &= G_2 \times G_4, \end{aligned} \quad (8)$$

with ρ_1 and ρ_2 denoting the correlation coefficients between the GG RVs, while ρ_G is the correlation coefficient of the dGG RVs. The joint PDF of R_1 and R_2 can be obtained by

$$f_{R_1, R_2}(x_1, x_2) = \int_0^\infty \int_0^\infty \frac{f_{G_1, G_2}(x, y)}{xy} f_{G_3, G_4} \left(\frac{x_1}{x}, \frac{x_2}{y} \right) dx dy, \quad (9)$$

with $f_{G_j, G_{j+1}}(x, y)$ denoting the joint GG PDF given by [21, Eq. (28)]

$$\begin{aligned} f_{G_j, G_{j+1}}(x, y) &= \frac{\beta_1 \beta_2 m_j^{m_j+1} x^{\frac{\beta_1}{2}(m_j+1)-1} y^{\frac{\beta_2}{2}(m_j+1)-1}}{\Gamma(m_j) \Omega_j^{\frac{m_j+1}{2}} \Omega_{j+1}^{\frac{m_j+1}{2}} (1-\rho_{f_1}) \rho_{f_1}^{\frac{m_j-1}{2}}} \\ &\times \exp \left[-\frac{m_j}{1-\rho_{f_1}} \left(\frac{x^{\beta_1}}{\Omega_j} + \frac{y^{\beta_2}}{\Omega_{j+1}} \right) \right] I_{m_j-1} \left[\frac{2m_j \sqrt{\rho_{f_1}} x^{\frac{\beta_1}{2}} y^{\frac{\beta_2}{2}}}{\sqrt{\Omega_j \Omega_{j+1}} (1-\rho_{f_1})} \right]. \end{aligned} \quad (10)$$

In (10), if $j = 1 \Rightarrow f_1 = 1$, else if $j = 3 \Rightarrow f_1 = 2$. Substituting (10) in (9) results into an integral representation for the bivariate dGG distribution. An alternative representation can be obtained by employing $I_\nu(z) = \sum_{h=0}^\infty \frac{(z/2)^{\nu+2h}}{h! \Gamma(\nu+h+1)}$ [22, Eq. (8.445)], making a change of variables of the form $t = x_1^2$, and using [22, Eq. (3.471/9)], yielding the following expression for the joint PDF of R_1 and R_2

$$\begin{aligned} f_{R_1, R_2}(x_1, x_2) &= \sum_{q_1, q_2=0}^\infty \prod_{t=1}^2 \frac{2\beta_t \rho_t^{q_t} / \Gamma(m_{f_2})}{q_t! (1-\rho_t)^{2p_3+m_{f_1}}} \\ &\times \frac{\hat{\Omega}_t^{p_1+p_3} x_t^{\beta_t(p_1+p_3)-1}}{\Gamma(m_{f_2} + q_t)} K_{2(p_2+p_4)} \left(2\sqrt{\frac{\hat{\Omega}_t}{\hat{\rho}}} x_t^{\frac{\beta_t}{2}} \right), \end{aligned} \quad (11)$$

with $p_3 = \frac{q_1+q_2}{2}$, $p_4 = \frac{q_2-q_1}{2}$, $\hat{\rho} = (1-\rho_1)(1-\rho_2)$, $\hat{\Omega}_2 = \frac{m_1 m_3}{\Omega_2 \Omega_4}$, $\Omega_{j+1} = (\mathbb{E} \langle G_{j+1}^2 \rangle \Gamma(m_j) / \Gamma(m_j + 2/\beta_2))^{1/\beta_2} m_j$. In (11), if $t = 1 \Rightarrow f_1 = 3, f_2 = 1$, else if $t = 2 \Rightarrow f_1 = 1, f_2 = 3$. Moreover, β_1, β_2 characterize R_1, R_2 , respectively, while m_1, m_2 are related with the first and second GG RVs, respectively, in both R_1, R_2 . By setting $m_1 = m_3 = 1, \beta_1 = \beta_2 = 2, \rho_1 = \rho_2, \Omega_1 = \Omega_2$, and $\Omega_3 = \Omega_4$, (11) simplifies to the joint PDF of the bivariate dR distribution given in [28, Eq. (6.69)].

For obtaining the corresponding joint CDF of R_1 and R_2 , the Meijer G-function representation of the Bessel function is employed, i.e., [29, Eq. (14)], and then using [29, Eq. (26)], the following generic expression can be obtained

$$\begin{aligned} f_{R_1, R_2}(x_1, x_2) &= \sum_{q_1, q_2=0}^\infty \prod_{t=1}^2 \frac{\rho_t^{q_t} / \Gamma(m_{f_2})}{(1-\rho_t)^{2p_3+m_{f_1}}} \frac{\hat{\Omega}_t^{p_1+p_3} / q_t!}{\Gamma(m_{f_2} + q_t)} \\ &\times x_t^{\beta_t(p_1+p_3)} \mathcal{G}_{1,3}^{2,1} \left(\frac{\hat{\Omega}_t}{\hat{\rho}} x_t^{\beta_t} \middle|_{p_2+p_4, -p_2-p_4, -p_1-p_3}^{1-p_1-p_3} \right). \end{aligned} \quad (12)$$

By setting $m_1 = m_3 = 1$ and $\beta_1 = \beta_2 = 2$, (12) simplifies to the joint CDF of the bivariate dR distribution given in [20, Eq. (6)]. Moreover, assuming $|m_3 - m_1| = n + 1/2$, employing [22, Eq. (8.468)], and then using [22, Eq. (8.350/1)], the following simplified expression for $F_{R_1, R_2}(x_1, x_2)$ is derived

$$\begin{aligned} F_{R_1, R_2}(x_1, x_2) &= 2\pi \sum_{q_1, q_2=0}^\infty \sum_{\ell_1, \ell_2=0}^{\phi(p_2, p_4)} \prod_{t=1}^2 \frac{2^{1-2(p_1+p_3)-\ell_t}}{\Gamma(m_{f_2}) q_t! \ell_t!} \\ &\times \frac{\rho_t^{q_t} (1-\rho_t)^{m_{f_2}} (\phi(p_2, p_4) + \ell_t)!}{\Gamma(m_{f_2} + q_t) (\phi(p_2, p_4) - \ell_t)!} \\ &\times \gamma \left(2(p_1 + p_3) - \ell_t - \frac{1}{2}, 2\sqrt{\frac{\hat{\Omega}_t}{\hat{\rho}}} x_t^{\frac{\beta_t}{2}} \right), \end{aligned} \quad (13)$$

in which $\phi(p_2, p_4) = 2|p_4 + p_2| - \frac{1}{2}$ and $\gamma(\cdot, \cdot)$ denotes the lower incomplete Gamma function [22, Eq. (8.350/1)].

In addition, based on (11) and with the aid of [22, Eq. (6.561/16)], the joint moments of R_1 and R_2 can be expressed as

$$\begin{aligned} \mathbb{E}\langle R_1^{n_1} R_2^{n_2} \rangle &= \sum_{q_1, q_2=0}^{\infty} \prod_{t=1}^2 \frac{\rho_t^{q_t} (1 - \rho_t)^{m_{f_2} + \frac{n_1}{\beta_1} + \frac{n_2}{\beta_2}} / \hat{\Omega}_t^{\frac{n_t}{\beta_t}}}{q_t! \Gamma(m_{f_2} + q_t) m_{f_2}^{\frac{n_3-t}{\beta_3-i}} \Gamma(m_{f_2})} \\ &\times \Gamma\left(k_t + m_{f_2} + \frac{n_1}{\beta_1}\right) \Gamma\left(k_t + m_{f_2} + \frac{n_2}{\beta_2}\right), \end{aligned} \quad (14)$$

which, by using the definition of the Gauss hypergeometric function [22, Eq. (9.100)], can be further simplified to the following closed-form expression

$$\begin{aligned} \mathbb{E}\langle R_1^{n_1} R_2^{n_2} \rangle &= \left[\prod_{t=1}^2 \frac{(1 - \rho_t)^{m_{f_2} + \frac{n_1}{\beta_1} + \frac{n_2}{\beta_2}}}{m_{f_2}^{\frac{n_3-t}{\beta_3-i}} \Gamma(m_{f_2}) 2 \hat{\Omega}_t^{\frac{n_t}{\beta_t}}} \Gamma\left(m_{f_2} + \frac{n_1}{\beta_1}\right) \right. \\ &\left. \times \Gamma\left(m_{f_2} + \frac{n_2}{\beta_2}\right) {}_2F_1\left(m_{f_2} + \frac{n_1}{\beta_1}, m_{f_2} + \frac{n_2}{\beta_2}; m_{f_2}; \rho_t\right) \right], \end{aligned} \quad (15)$$

with ${}_2F_1(\cdot, \cdot; \cdot; \cdot)$ denoting the Gauss hypergeometric function [22, Eq. (9.100)]. By definition, the power correlation coefficient between R_1 and R_2 , ρ_G , is given by

$$\rho_G = \frac{\text{cov}(R_1^2, R_2^2)}{\sqrt{\text{var}(R_1^2) \text{var}(R_2^2)}}, \quad (16)$$

with $\text{cov}(\cdot)$ denoting covariance and $\text{var}(\cdot)$ variance. Substituting (7) and (15) in this definition and doing some mathematical manipulations yield the following expression for ρ_G

$$\begin{aligned} \rho_G &= \prod_{j=1}^2 \frac{\Gamma(m_1 + \frac{2}{\beta_j}) \Gamma(m_3 + \frac{2}{\beta_j})}{\left[\prod_{t=1}^2 \Gamma\left(m_{f_2} + \frac{4}{\beta_j}\right) \Gamma(m_{f_2}) - \prod_{t=1}^2 \Gamma\left(m_{f_2} + \frac{2}{\beta_j}\right)^2 \right]^{\frac{1}{2}}} \\ &\times \left[\prod_{t=1}^2 (1 - \rho_t)^{m_{f_2} + \frac{2}{\beta_1} + \frac{2}{\beta_2}} \right. \\ &\left. \times {}_2F_1\left(m_{f_2} + \frac{2}{\beta_1}, m_{f_2} + \frac{2}{\beta_2}; m_{f_2}; \rho_t\right) - 1 \right]. \end{aligned} \quad (17)$$

It is noteworthy that by setting $m_1 = m_3 = 1$ in (17), it simplifies to a previous known result [26, Eq. (10)].

C. Second-Order Statistics

Let $R(t)$ be a dGG process with marginal and bivariate PDFs given by (3) and (11), respectively. Moreover, let \dot{R} denote the time derivative of R , i.e., $\dot{R}(t) = dR(t)/dt$, at time t . Since the dGG random process is a product of two independent GG random processes, i.e., $R(t) = G_1(t)G_3(t)$, the joint PDF of $R(t)$ and $\dot{R}(t)$ can be expressed as [30]

$$f_{R\dot{R}}(x, \dot{x}) = \int_0^{\infty} \int_{-\infty}^{\infty} \frac{1}{y^2} f_{G_1\dot{G}_1}\left(\frac{x}{y}, \frac{\dot{x}}{y} - \frac{\dot{y}x}{y^2}\right) f_{G_3\dot{G}_3}(y, \dot{y}) d\dot{y} dy, \quad (18)$$

with $f_{G_j\dot{G}_j}(\cdot, \cdot)$ representing the joint PDF of the GG random process $G_j(t)$ and its derivative $\dot{G}_j(t)$, which is given in [21, Eq. (24)]. Assuming $\beta_1 = \beta_2 = \beta$, $m_1 = m_3 = m$, $\Omega_1 = \Omega_3 = \Omega$, substituting [21, Eq. (24)] in (18), using [22, Eq. (3.323/2)], and performing some mathematical manipulations, the following expression for the joint PDF of $R(t)$ and $\dot{R}(t)$ is deduced

$$\begin{aligned} f_{R\dot{R}}(x, \dot{x}) &= \frac{\beta^2 m^{2m+0.5} x^{\beta(m+0.5)-2}}{\sqrt{2\pi\omega\Omega^{2m+0.5}} \Gamma(m)^2} \\ &\times \int_0^{\infty} \frac{y^{-1} \exp\left(-\frac{m}{\Omega} y\right)}{\sqrt{x^{\beta} y^{-1} + y}} \exp\left[\frac{m\beta^2 \dot{x}^2 x^{2\beta-2}}{(x^{\beta} + y^2) 2\omega^2 \Omega y}\right] \\ &\times \exp\left[-\frac{mx^{\beta}}{\Omega} \left(\frac{\beta^2 \dot{x}^2}{2\omega^2 x^2} + 1\right) y^{-1}\right] dy, \end{aligned} \quad (19)$$

in which ω denotes frequency in radians per second.

1) *Level Crossing Rate*: LCR is defined as the number of times per unit duration that a random process crosses a predefined threshold (R_{th}) in the negative direction, and is mathematically given by [31]

$$N_R(R_{\text{th}}) = \int_0^{\infty} \dot{x} f_{R\dot{R}}(R_{\text{th}}, \dot{x}) d\dot{x}. \quad (20)$$

Substituting (19) in (20) and using [22, Eq. (3.310)] yield

$$\begin{aligned} N_R(R_{\text{th}}) &= \frac{m^{2m-0.5} \omega R_{\text{th}}^{\beta(m-0.5)}}{\sqrt{2\pi\Omega^{2m-0.5}} \Gamma(m)^2} \int_0^{\infty} \frac{y^{-3/2}}{\sqrt{R_{\text{th}}^{\beta} + y^2}} \\ &\times \exp\left(-\frac{m}{\Omega} y\right) \exp\left(-\frac{mR_{\text{th}}^{\beta}}{\Omega} y^{-1}\right) (y^2 + R_{\text{th}}^{\beta}) dy. \end{aligned} \quad (21)$$

Assuming $\beta = 2$, (21) simplifies to the LCR of the dN distribution derived in [7, Eq. (9)].

2) *Average Fade Duration*: Assuming that $R(t)$ models the envelope of the fading channel, the AFD is defined as the average length of time the envelope remains under R_{th} , once it crosses this value in the negative direction. It can be expressed mathematically as [31]

$$\alpha(R_{\text{th}}) = \frac{F_R(R_{\text{th}})}{N_R(R_{\text{th}})}, \quad (22)$$

in which $F_R(R_{\text{th}})$ and $N_R(R_{\text{th}})$ are given by (4) and (21), respectively. By setting $\beta = 2$ in (22), it simplifies to the AFD of the dN distribution as derived in [7, Eq. (10)]. It should be noted that most of the above-derived expressions have never been reported in the open technical literature.

III. TAS STATISTICS

A. System Model

In order to satisfy the space and hardware limitation constraints existing in VANETs, we consider a communication system where the transmitter (equipped with L antennas) employs one RF chain opportunistically with a single-antenna receiver. This system operates in a V2V communication environment subject to fading that is modelled by the dGG distribution. The overall TAS scheme is carried out in two phases: the selection phase and the transmission phase. More

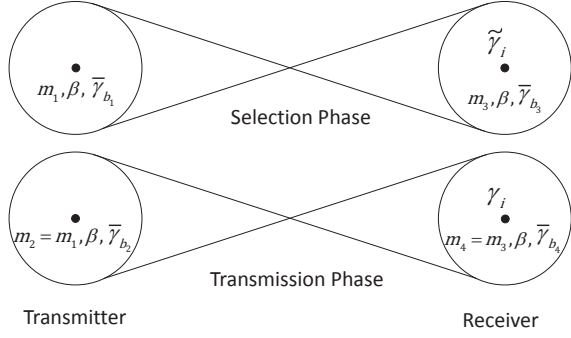


Fig. 1. Double-scattering propagation and parameters for each bounce in transmit antenna i .

specifically, the transmit antenna providing the highest received SNR value is selected at the receiver. This information is communicated to the transmitter via an error-free feedback link. Assuming identical parameters for all diversity links, the instantaneous received output SNR can be expressed as

$$\gamma_{\text{out}} = \max\{\gamma_1, \gamma_2, \dots, \gamma_L\}, \quad (23)$$

in which $\gamma_i = R_i^2 \frac{E_s}{N_0}$ is associated with the i th ($i \in \{1, \dots, L\}$) transmitting antenna, R_i being the distributed fading amplitude following the PDF given in (3), E_s the transmitted symbol energy, and N_0 the noise variance. The corresponding PDF and CDF of γ_i are, respectively, given by

$$f_{\gamma_i}(\gamma) = \frac{\beta \hat{\gamma}_1^{\frac{m_1+m_3}{2}}}{\Gamma(m_1) \Gamma(m_3)} \times \gamma^{\frac{\beta}{4}(m_1+m_3)-1} K_{m_3-m_1} \left(2\sqrt{\hat{\gamma}_1} \gamma^{\frac{\beta}{4}} \right), \quad (24)$$

$$F_{\gamma_i}(\gamma) = \frac{1}{\Gamma(m_3)} \left[1 - \sum_{k_1, k_2=0}^{\zeta(m_1, m_3)} D_1 \hat{\gamma}_1^{\frac{k_1+m_1-k_2-1/2}{2}} \times \gamma^{\frac{\beta}{4}(k_1+m_1-k_2-1/2)} \exp \left(-2\sqrt{\hat{\gamma}_1} \gamma^{\frac{\beta}{4}} \right) \right], \quad (25)$$

with $\hat{\gamma}_t = \left[\frac{\Gamma(m_1) \Gamma(m_3) \bar{\gamma}_{b_t} \bar{\gamma}_{b_{t+2}}}{\Gamma(m_1+2/\beta) \Gamma(m_3+2/\beta)} \right]^{-\frac{\beta}{2}}$ and $\bar{\gamma} = \mathbb{E} \langle R_i^2 \rangle \frac{E_s}{N_0} = \bar{\gamma}_{b_t} \bar{\gamma}_{b_{t+2}}$, in which $t \in \{1, 2\}$.

It is noteworthy that in the past, the performance of similar communication systems has been studied based on i) special cases regarding the double-scattering propagation, i.e., using dR and dN fading distributions, and ii) ideal conditions regarding the CSI acquisition, e.g., [10], [17]. As far as channel modeling is concerned, capitalizing on the generic form of the dGG distribution, the accurate modeling of several double-bounce fading conditions is allowed. More specifically, in (24), m_j, β are related with the severity of the fading, i.e., lower values for m_j, β denote severe fading conditions. In Fig. 1, for clarification purposes, the shaping and scaling parameters of the constitute GG fading distributions, for each bounce and communication phase, are depicted. As far as CSI feedback delay is concerned, two scenarios have been examined, one with ideal and one with non-ideal feedback, due to the impact of outdated CSI.

B. Ideal Feedback

For the system under consideration and under the assumption of no feedback delay, i.e., ideal feedback, the CDF of γ_{out} is given by following order statistics with L independent RVs as

$$F_{\gamma_{\text{out}}}(\gamma) = [F_{\gamma_i}(\gamma)]^L. \quad (26)$$

Using (25) in (26), employing first the binomial identity, then multinomial identity, and after some mathematical procedure, the following convenient closed-form expression for $F_{\gamma_{\text{out}}}(\gamma)$ is attained

$$F_{\gamma_{\text{out}}}(\gamma) = \sum_{q, t_i, v_{i,j}}^L \frac{\binom{L}{q}}{\Gamma(m_3)^L} D_2 \hat{\gamma}_1^{d_2} \gamma^{\frac{\beta d_2}{2}} \exp \left(-2q \hat{\gamma}_1^{1/2} \gamma^{\frac{\beta}{4}} \right), \quad (27)$$

with

$$\sum_{q, t_i, v_{i,j}}^L = \sum_{q=0}^L \sum_{\substack{t_1, \dots, t_{m_3}=0 \\ t_1 + \dots + t_{m_3} = q}}^q \dots \sum_{\substack{v_{1,1}, \dots, v_{m_3, |m_3-1-m_1|-\frac{1}{2}}=0 \\ v_{1,1} + \dots + v_{m_3, |m_3-1-m_1|-\frac{1}{2}} = t_{m_3}}}^{t_{m_3}},$$

$$D_2 = \frac{(-1)^q q!}{t_1! \dots t_{m_3}!} \left[\frac{\sqrt{\pi}}{\Gamma(m_1)} \right]^q \times \frac{t_1! \dots t_{m_3}!}{v_{1,1}! \dots v_{1, m_1+\frac{1}{2}}! \dots v_{m_3, 1}! \dots v_{m_3, |m_3-1-m_1|-\frac{1}{2}}!} \times \prod_{k=0}^{m_3-1} \prod_{p=0}^{|k-m_1|-\frac{1}{2}} \left[\frac{(|k-m_1|-\frac{1}{2}+p)!}{k! p! (|k-m_1|-\frac{1}{2}-p)! 2^{2p}} \right]^{v_{k+1, p+1}},$$

and

$$d_2 = \sum_{k=0}^{m_3-1} \sum_{p=0}^{|k-m_1|-\frac{1}{2}} \left(\frac{k+m_1-p-1/2}{2} \right) v_{k+1, p+1}.$$

The corresponding PDF expression is given by $f_{\gamma_{\text{out}}}(\gamma) = L f_{\gamma_i}(\gamma) F_{\gamma_i}(\gamma)^{L-1}$. Substituting (27) in this expression and doing some mathematical manipulations yield the following expression for the PDF of γ_{out}

$$f_{\gamma_{\text{out}}}(\gamma) = L f_{\gamma_i}(\gamma) \sum_{q, t_i, v_{i,j}}^{L-1} \frac{1}{\Gamma(m_3)^{L-1}} \binom{L-1}{q} \times D_2 \hat{\gamma}_1^{d_2} \gamma^{\frac{\beta d_2}{2}} \exp \left(-2q \hat{\gamma}_1^{1/2} \gamma^{\frac{\beta}{4}} \right). \quad (28)$$

It is noteworthy that both eqs. (27) and (28) are presented for the first time.

C. Non-Ideal Feedback

In fast fading environments, due to the continuous motion of the transmitter and/or the receiver, as it is the case in V2V communications, it is very likely that the fading amplitude will vary fast [32]. Hence, in many cases, the decision for the antenna selection will be based on outdated CSI due to the feedback delay between the antenna selection and data transmission phases. In this context, the impact of outdated CSI is investigated using the correlation model adopted by many authors in the past, e.g., [33]. More specifically, the discrepancy between the actual SNR of the i th antenna for

data transmission, γ_i , and the one that is available during the selection phase, $\tilde{\gamma}_i$, can be characterized based on the correlation coefficient ρ_G . In this case, the PDF of the actual received SNR of the *selected* antenna at the data transmission instance can be expressed as

$$f_{\gamma_{\text{out}}}(\gamma) = \int_0^\infty f_{\gamma_i, \tilde{\gamma}_i}(\gamma, x) \frac{f_{\tilde{\gamma}_{\text{out}}}(x)}{f_{\gamma_i}(x)} dx, \quad (29)$$

in which $f_{\tilde{\gamma}_{\text{out}}}(x)$ is given by (28) and $f_{\gamma_i, \tilde{\gamma}_i}(\gamma, x)$ can be easily evaluated, by applying a change of variables in (11), as

$$f_{\gamma_i, \tilde{\gamma}_i}(\gamma, x) = \sum_{q_1, q_2=0}^{\infty} \mathcal{P} \gamma^{\frac{\beta}{2}(p_1+p_3)-1} x^{\frac{\beta}{2}(p_1+p_3)-1} \times K_{2(p_2+p_4)} \left(2\sqrt{\frac{\hat{\gamma}_1}{\hat{\rho}}} \gamma^{\frac{\beta}{4}} \right) K_{2(p_2+p_4)} \left(2\sqrt{\frac{\hat{\gamma}_2}{\hat{\rho}}} x^{\frac{\beta}{4}} \right), \quad (30)$$

with $\mathcal{P} = \left[\prod_{t=1}^2 \frac{\beta \rho_t^{q_t} / \Gamma(m_{f_2})}{(1-\rho_t)^{2p_3+m_{f_1}} q_t! \Gamma(m_{f_2}+q_t)} \frac{\hat{\gamma}_t^{p_1+p_3}}{q_t! \Gamma(m_{f_2}+q_t)} \right]$. In Appendix A, it has been proved that the PDF of the output SNR, when outdated CSI is assumed to be available, is given by

$$f_{\gamma_{\text{out}}}(\gamma) = \sum_{q_1, q_2=0}^{\infty} \sum_{q, t_i, v_i, j}^{L-1} \frac{L\mathcal{P}}{\Gamma(m_3)^{L-1}} \binom{L-1}{q} \frac{D_2}{\hat{\gamma}_2^{p_1+p_3}} \times D_3 \gamma^{\frac{\beta}{2}(p_1+p_3)-1} K_{2(p_2+p_4)} \left(2\sqrt{\frac{\hat{\gamma}_1}{\hat{\rho}}} \gamma^{\frac{\beta}{4}} \right). \quad (31)$$

Based on (31), for evaluating the corresponding CDF expression, an integral of the following form should be solved

$$Q(\gamma) = \int_0^\gamma \gamma^{\frac{\beta}{2}(p_1+p_3)-1} K_{2(p_2+p_4)} \left(2\sqrt{\frac{\hat{\gamma}_1}{\hat{\rho}}} \gamma^{\frac{\beta}{4}} \right) d\gamma. \quad (32)$$

Making a change of variables in (32), using [34, Eq. (1.12.1/2)], and after some mathematical simplifications, the following closed-form expression for \mathcal{I}_2 is extracted

$$Q(\gamma) = \frac{\pi}{\beta} \frac{\gamma^{\frac{\beta}{2}(q_1+m_1)} (\hat{\rho}/\hat{\gamma}_1)^{p_2+p_4}}{\sin[2\pi(p_2+p_4)]} \left[\Gamma(q_1+m_1) \times {}_1\tilde{F}_2 \left(q_1+m_1; 1-2(p_2+p_4), q_1+m_1+1; \frac{\hat{\gamma}_1 \gamma^{\frac{\beta}{2}}}{\hat{\rho}} \right) - \left(\frac{\hat{\gamma}_1 \gamma^{\frac{\beta}{2}}}{\hat{\rho}} \right)^{2(p_2+p_4)} \Gamma(q_2+m_3) \times {}_1\tilde{F}_2 \left(q_2+m_3; 1+2(p_2+p_4), q_2+m_3+1; \frac{\hat{\gamma}_1 \gamma^{\frac{\beta}{2}}}{\hat{\rho}} \right) \right], \quad (33)$$

in which ${}_1\tilde{F}_2(\cdot; \cdot, \cdot; \cdot)$ denotes the regularized generalized hypergeometric function [35, Eq. (07.32.02.0001.01)]. Based on (33) and after some mathematical simplifications, the following expression for the CDF of γ_{out} is obtained

$$F_{\gamma_{\text{out}}}(\gamma) = \sum_{q_1, q_2=0}^{\infty} \sum_{q, t_i, v_i, j}^{L-1} \frac{L\mathcal{P}}{\Gamma(m_3)^{L-1}} \binom{L-1}{q} \frac{D_2}{\hat{\gamma}_2^{p_1+p_3}} \times D_3 Q(\gamma). \quad (34)$$

Here, it is considered essential to investigate the rate of convergence of the infinite series given in (34). In particular,

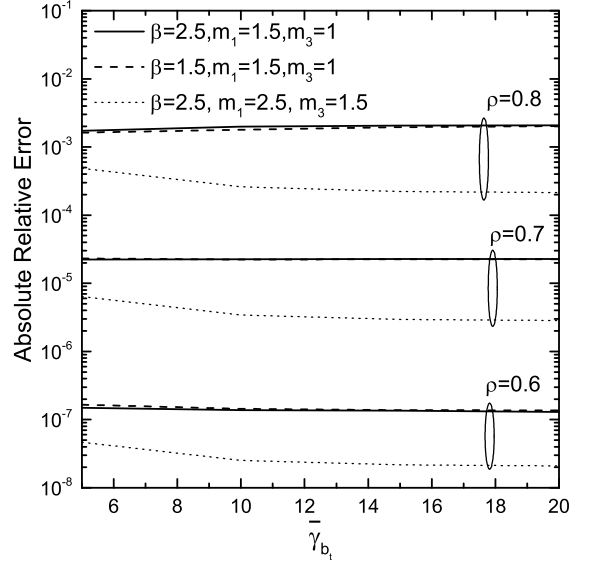


Fig. 2. Absolute relative error of (34) after the truncation of the first 30 terms.

in Fig. 2, assuming $\gamma = 1$, the absolute relative errors ϵ of the CDF expression given in (34) is evaluated. This error is defined as $\epsilon = |F_1 - F_2|/F_1$, with F_1 representing the exact value of the CDF and F_2 representing the corresponding value of the CDF after the truncation of the first 30 terms. In this figure, it is shown that ϵ depends on $\rho = \rho_1 = \rho_2$, $\bar{\gamma}_{b_t}$, β , m_j , with the first one having dominant influence. It is noteworthy that in all cases with a small number of terms, an excellent accuracy is achieved. It should be also noted that similar rates of convergence have been also observed for all the infinite series expressions presented in this paper.

D. Asymptotic Analysis

The exact expressions for $F_{\gamma_{\text{out}}}(\gamma)$ for both feedback scenarios do not provide a direct physical insight of the system's performance. In order to simplify the analysis, the main concern is to derive asymptotic *closed-form* expressions for $F_{\gamma_{\text{out}}}(\gamma)$.

1) *Ideal Feedback*: Assuming high values of $\bar{\gamma}_{b_t}$, using $\gamma(a, z_1) \simeq z_1^a$ (for small z_1) [35, Eq. (06.07.06.0004.01)], and after some mathematical manipulations, the following closed-form asymptotic expression for the CDF of γ_{out} is derived

$$F_{\gamma_{\text{out}}}(\gamma) \simeq \left(\frac{\Gamma(m_1 - m_3) \gamma^{\frac{\beta}{2} m_3} \hat{\gamma}_1^{m_3}}{\Gamma(m_1) \Gamma(m_3) m_3} \right)^L. \quad (35)$$

2) *Non-Ideal Feedback*: Assuming high values of the average SNR, using $I_\nu(z) \simeq \frac{(z/2)^\nu}{\Gamma(\nu+1)}$ (for small z) [35, Eq. (03.02.06.0004.01)], and after some mathematical manipulations, (30) simplifies to the following closed-form expression

$$f_{\gamma_i, \tilde{\gamma}_i}(\gamma, x) \simeq \frac{\beta^2 \gamma^{\frac{\beta}{4}(m_1+m_3)-1} x^{\frac{\beta}{4}(m_1+m_3)-1} / \Gamma(m_1)^2}{\Gamma(m_3)^2 (\hat{\gamma}_1 \hat{\gamma}_2)^{-\frac{m_1+m_3}{2}} (1-\rho_1)^{m_3} (1-\rho_2)^{m_1}} \times K_{2p_2} \left(2\sqrt{\frac{\hat{\gamma}_1}{\hat{\rho}}} \gamma^{\frac{\beta}{4}} \right) K_{2p_2} \left(2\sqrt{\frac{\hat{\gamma}_2}{\hat{\rho}}} x^{\frac{\beta}{4}} \right). \quad (36)$$

Furthermore, assuming $\rho = \rho_1 = \rho_2$, substituting (36) and the derivative of (35) in (29), using $K_v(z) \simeq \frac{1}{2}\Gamma(v) \left(\frac{1}{2}z\right)^{-v}$ (for small z) [24, Eq. (9.6.9)], and after some mathematical procedure, yield the following closed-form expression for the CDF of the output SNR

$$F_{\gamma_{\text{out}}}(\gamma) \simeq \frac{L\Gamma(m_1 - m_3)^L \Gamma(Lm_3) \hat{\gamma}_1^{m_3}}{(1 - \rho)^{3m_3 - m_1 - 2Lm_3} m_3^L} \times \frac{\Gamma(m_1 + (L - 1)m_3)}{[\Gamma(m_1)\Gamma(m_3)]^{L+1}} \gamma^{\beta m_3/2}. \quad (37)$$

IV. PERFORMANCE ANALYSIS

In this section, using the previously derived results, analytical expressions for important performance metrics such as the OP, the SEP, the average capacity, the LCR, and the AFD are derived.

A. Outage Probability (OP)

OP is defined as the probability that the output SNR falls below a predetermined threshold γ_T and is given by $P_{\text{out}} = F_{\gamma_{\text{out}}}(\gamma_T)$, which $F_{\gamma_{\text{out}}}(\gamma_T)$ can be evaluated using (27), for the ideal feedback scenario, and (34), for the non-ideal feedback scenario.

Diversity and Coding Gains: At the high SNR regime, the OP can be characterized by two parameters, viz., diversity gain G_d and coding gain G_c , as $P_{\text{out}}^\infty \simeq (G_c \bar{\gamma}_{b_i})^{-G_d}$. In this context, for the ideal feedback scenario and based on (35), it can be inferred that

$$G_C = \left[\frac{\Gamma(m_1 - m_3) [\Gamma(m_1 + 2/\beta) \Gamma(m_3 + 2/\beta)]^{m_3} \frac{\beta}{2} \gamma_T^{\frac{\beta}{2} m_3}}{[\Gamma(m_1)\Gamma(m_3)]^{m_3} \frac{\beta}{2} + 1 m_3} \right]^{-1/(m_3\beta)}$$

and $G_d = m_3\beta L$. Therefore, for the ideal feedback scenario, the diversity gain depends on fading severity, modelled by the shaping parameters m_3, β , as well as the number of transmit antennas L . However, for non-ideal feedback scenario, based on (37), it results that $G_C =$

$$\left[\frac{L\Gamma(m_1 - m_3)^L \Gamma(Lm_3) \Gamma(m_1 + (L - 1)m_3) \Gamma(m_1 + \frac{2}{\beta})^{\frac{\beta}{2} m_3} \Gamma(m_3 + \frac{2}{\beta})^{\frac{\beta}{2} m_3}}{\Gamma(m_1)^{\frac{\beta m_3}{2} + L + 1} \Gamma(m_3)^{\frac{\beta m_3}{2} + L + 1} (1 - \rho)^{3m_3 - m_1 - 2Lm_3} m_3^L} \right]^{-1/(m_3\beta)}$$

and $G_d = m_3\beta$. Thus, the outdated feedback has a detrimental effect on the OP performance, since the desired diversity gain $G_d = m_3\beta L$ is not realized.

B. Symbol Error Probability (SEP)

The SEP is one of the most important performance measures, the minimization of which is the main objective in designing wireless communication systems.

1) *Ideal Feedback:* For evaluating the SEP, the CDF-based approach is employed as follows [36]

$$\bar{P}_e = \int_0^\infty (-P_e') F_{\gamma_{\text{out}}}(\gamma) d\gamma, \quad (38)$$

with $(-P_e')$ denoting the negative derivative of the conditional error probability. In particular, for binary phase shift keying (BPSK) or binary frequency shift keying (BFSK) $P_e = \alpha Q(\sqrt{b\gamma})$, while for differentially BPSK (DBPSK) $P_e = \alpha \exp(-b\gamma)$. As far as BPSK scheme is concerned,

the following closed-form expression for the SEP has been obtained

$$\bar{P}_e = \sum_{q, t_i, v_i, j}^L \frac{1}{\Gamma(m_3)^L} \binom{L}{q} D_2 \hat{\gamma}_1^{d_2} \frac{\alpha \sqrt{b}}{\sqrt{8\pi}} D_4 \left(\frac{b}{2}, \frac{1}{2} \right). \quad (39)$$

The proof as well as D_4 are given in Appendix B. It is noted that (39) generalizes previous known result [9, Eq. (20)]. For the DBPSK scheme, by following a similar approach as the one used for deriving the SEP of BPSK, the following expression is deduced

$$\bar{P}_e = \sum_{q, t_i, v_i, j}^L \frac{1}{\Gamma(m_3)^L} \binom{L}{q} D_2 \hat{\gamma}_1^{d_2} ab D_4(b, 1). \quad (40)$$

2) *Non-Ideal Feedback:* For this scenario, in order to evaluate the SEP, the PDF-based approach will be employed as follows

$$\bar{P}_e = \int_0^\infty P_s f_{\gamma_{\text{out}}}(\gamma) d\gamma, \quad (41)$$

with P_s denoting the conditional SEP. More specifically, for BPSK and BFSK $P_s = A \text{erfc}(\sqrt{B\gamma})$, with $\text{erfc}(\cdot)$ denoting the complementary error function [22, Eq. (8.25/4)], while for DBPSK $P_s = A \exp(-B\gamma)$. For BPSK and BFSK, the following expression for the SEP is derived

$$\bar{P}_e = \sum_{q_1, q_2=0}^\infty \sum_{q, t_i, v_i, j}^{L-1} \frac{LP}{\Gamma(m_3)^{L-1}} \binom{L-1}{q} \frac{AD_2}{\hat{\gamma}_1^{p_1+p_3}} D_3 D_5. \quad (42)$$

The proof as well as D_3, D_5 are provided in Appendix C. For DBPSK, the following expression for the SEP is obtained

$$\bar{P}_e = \sum_{q_1, q_2=0}^\infty \sum_{q, t_i, v_i, j}^{L-1} \frac{LP}{\Gamma(m_3)^{L-1}} \binom{L-1}{q} \frac{AD_2}{\hat{\gamma}_1^{p_1+p_3}} D_3 D_6. \quad (43)$$

The proof as well as D_6 are provided in Appendix C.

C. Average Channel Capacity

Average channel capacity is defined as

$$\hat{C} = BW \int_0^\infty \log_2(1 + \gamma) f_{\gamma_{\text{out}}}(\gamma) d\gamma \quad (44a)$$

$$= \frac{BW}{\ln(2)} \int_0^\infty \frac{1 - F_{\gamma_{\text{out}}}(\gamma)}{1 + \gamma} d\gamma, \quad (44b)$$

with BW denoting the signal's transmission bandwidth.

1) *Ideal Feedback:* For the ideal feedback case, the following closed-form expression has been derived for the capacity

$$\hat{C} = \sum_{q, t_i, v_i, j}^L \frac{BW(-1)^{-1}}{\ln(2)\Gamma(m_3)^L} \binom{L}{q} D_2 \hat{\gamma}_1^{d_2} D_7, \quad (45)$$

with q starting at 1. The proof and D_7 are given in Appendix B.

2) *Non-Ideal Feedback*: For the non-ideal feedback case, the following expression has been derived for the capacity

$$\hat{C} = L \sum_{q_1, q_2=0}^{\infty} \mathcal{P} \sum_{q, t_i, v_{i,j}}^{L-1} \frac{BW/\ln(2)}{\Gamma(m_3)^{L-1}} \binom{L-1}{q} \frac{D_2}{\hat{\gamma}_1^{p_1+p_3}} D_3 D_8. \quad (46)$$

The proof and D_8 are provided in Appendix C.

D. Average Output SNR

The average output SNR is a performance metric providing excellent indication of the overall system's fidelity. For the scheme under consideration, it is defined as

$$\mathbb{E}\langle \gamma_{\text{out}} \rangle = \int_0^{\infty} \gamma f_{\gamma_{\text{out}}}(\gamma) d\gamma \quad (47a)$$

$$= \int_0^{\infty} [1 - F_{\gamma_{\text{out}}}(\gamma)] d\gamma. \quad (47b)$$

1) *Ideal Feedback*: Substituting (27) in (47b), using [22, Eq. (3.351/3)], and after some mathematical simplifications, the following expression is deduced

$$\mathbb{E}\langle \gamma_{\text{out}} \rangle = \sum_{q, t_i, v_{i,j}}^L \frac{(-1)^{-1}}{\Gamma(m_3)^L} \binom{L}{q} D_2 \frac{2^{2-\frac{4}{\beta}-2d_2} \Gamma\left(\frac{4}{\beta} + 2d_2\right)}{\beta \hat{\gamma}_1^{\frac{2}{\beta}} q^{\frac{2(2+\beta d_2)}{\beta}}}, \quad (48)$$

with q starting at 1.

2) *Non-Ideal Feedback*: Substituting (31) in (47a) and using [22, Eq. (6.561/16)], yield the following expression

$$\begin{aligned} \mathbb{E}\langle \gamma_{\text{out}} \rangle &= \sum_{q_1, q_2=0}^{\infty} \sum_{q, t_i, v_{i,j}}^{L-1} \frac{L\mathcal{P}}{\Gamma(m_3)^{L-1}} \binom{L-1}{q} \frac{D_2}{\hat{\gamma}_1^{p_1+p_3}} \frac{D_3}{\beta} \\ &\times \left(\frac{\hat{\rho}}{\hat{\gamma}_1}\right)^{\frac{2}{\beta}+p_1+p_3} \Gamma\left(\frac{2}{\beta} + m_1 + q_1\right) \Gamma\left(\frac{2}{\beta} + m_3 + q_2\right). \end{aligned} \quad (49)$$

E. Level Crossing Rate and Average Fade Duration

1) *Level Crossing Rate (LCR)*: The LCR for the system under consideration and threshold value R_{th} , is defined as the rate at which the system status changes from the non-outage to the outage status.

a) *Ideal Feedback*: Assuming independent and identically distributed fading conditions and using (21) as well as (4), the LCR can be evaluated as [31]

$$N_T(R_{\text{th}}) = LN_R(R_{\text{th}})F_R(R_{\text{th}})^{L-1}. \quad (50)$$

It is noted that by setting $\beta = 2$, (50) simplifies to LCR of dN fading process in TAS systems [8, Eq. (14)]. Moreover, since $R(t)$ denotes a fading process, ω denotes the maximum Doppler shift in radians per second, which depends on the speed of vehicle and the carrier frequency. For example, in a real-world example, assuming ITS-G5 standard and a vehicle speed equal to 80 km/h, $\omega = 2745.75$ rad/s. In addition, a simpler expression for N_R can be extracted for higher values of Ω . In particular, based on (19), using [22, Eq.

(3.351/3)] as well as [37, Eq. (2.3.7/8)], the following closed-form approximated expression for the LCR is obtained

$$\begin{aligned} N_R(R_{\text{th}}) &\simeq \left(\frac{m^m/\sqrt{\pi}}{\Omega^m \Gamma(m)}\right)^2 \sqrt{\Omega/(2m)} \omega R_{\text{th}}^{\beta(m-1/4)} \\ &\times \left[\frac{2\pi\Omega^{1/2} {}_1F_2\left(\frac{1}{2}; \frac{1}{4}, \frac{3}{4}; -\frac{m^2 R_{\text{th}}^{\beta}}{4\Omega^2}\right)}{\sqrt{m R_{\text{th}}^{\frac{\beta}{2}}}} \right. \\ &- 4\Gamma\left(\frac{3}{4}\right)^2 {}_1F_2\left(\frac{3}{4}; \frac{1}{2}, \frac{5}{4}; -\frac{m^2 R_{\text{th}}^{\beta}}{4\Omega^2}\right) \\ &\left. - \frac{m R_{\text{th}}^{\frac{\beta}{2}} \Gamma\left(-\frac{3}{4}\right) \Gamma\left(\frac{5}{4}\right) {}_1F_2\left(\frac{5}{4}; \frac{3}{2}, \frac{7}{4}; -\frac{m^2 R_{\text{th}}^{\beta}}{4\Omega^2}\right)}{\Omega} \right], \end{aligned} \quad (51)$$

with ${}_1F_2(\cdot; \cdot, \cdot; \cdot)$ denoting the generalized hypergeometric function [35, Eq. (07.22.02.0001.01)].

b) *Non-Ideal Feedback*: Since the system's outage depends on the correlation between two dGG RVs, which is mathematically described by (13), using this expression as well as the approach followed for deriving (34), the LCR can be expressed as

$$N_T(R_{\text{th}}) = LN_R(R_{\text{th}})F_{R_o, L-1}(R_{\text{th}}). \quad (52)$$

in which $F_{R_o, L-1}(R_{\text{th}}) = F_{\gamma_{\text{out}}}(\sqrt{R_{\text{th}}})$ given in (34), with $\hat{\gamma}_t$ substituted by $\hat{\Omega}_t$ and L by $L-1$.

2) Average Fade Duration (AFD):

a) *Ideal Feedback*: Based on (22) and using (50), AFD can be expressed as

$$a_T(R_{\text{th}}) = \frac{F_R(R_{\text{th}})^L}{LN_R(R_{\text{th}})F_R(R_{\text{th}})^{L-1}} = \frac{F_R(R_{\text{th}})}{LN_R(R_{\text{th}})}. \quad (53)$$

It is noted that by setting $\beta = 2$, (53) simplifies to AFD of dN fading process in TAS systems [8, Eq. (19)].

b) *Non-Ideal Feedback*: Based on (22) and using (52), AFD can be expressed as

$$a_T(R_{\text{th}}) = \frac{F_{R_o, L}(R_{\text{th}})}{LN_R(R_{\text{th}})F_{R_o, L-1}(R_{\text{th}})}, \quad (54)$$

in which $F_{R_o, L-1}(R_{\text{th}})$ and $F_{R_o, L}(R_{\text{th}})$ can be evaluated using (34).

V. NUMERICAL RESULTS

In this section, several numerically evaluated performance results are provided. These results include performance comparisons of several TAS structures, employing various modulation formats, and different V2V channel conditions. Furthermore, in order to obtain realistic values for the correlation coefficients between the exact and outdated values of the SNR, their range are evaluated using the following real-world example. Based on the ITS-G5 standard, with center frequency 5.9 GHz and varying vehicle speed $v = 10 - 40$ m/s, it will result to maximum Doppler frequency $f_D \approx 100 - 786$ Hz. In this example, the corresponding channel coherence time, which quantifies how fast the channel is changing over time, is $T_c \approx 200 - 1600$ μsec . Thus, as is also observed in [38], the coherence time of a vehicular channel could be less than

the duration of a 1kB packet. Assuming the classic Jakes spectrum, the autocorrelation function between the current and past states of the channel is given by $\rho_j = J_0(2\pi f_D T)$, with T denoting the time delay due to the CSI feedback and $J_v(\cdot)$ the first kind Bessel function [22, Eq. (8.402)]. Moreover, for simplicity and similar to [39], the time delay is considered to be equal to $T \approx [1/3 - 1]T_c$. In this example, the resulting range of values for the correlation coefficient will be $\rho_j \approx \{0.75 - 0.97\}$. It is noted that in this section similar range of values have been also considered for ρ_1, ρ_2 .

In Fig. 3, the OP is plotted as a function of $\bar{\gamma}_{b_t}$ for different values of the shaping parameter β and for both scenarios regarding feedback acquisition. The following parameters were set: $\rho_1 = 0.75$, $\rho_2 = 0.8$, $m_1 = 1.5$, $m_3 = 1$, $L = 3$, $\gamma_T = 0$ dB. It is shown that the performance improves with the increase of β , i.e., decrease of the fading severity, and/or $\bar{\gamma}_{b_t}$. In the same figure, the asymptotic performance of the OP is also plotted and is shown to be well aligned to the exact one in the high SNR region. Moreover, in this figure, the difference between the diversity gains of ideal and non-ideal feedback scenarios is clearly depicted. In addition, for the non-ideal feedback case and for $\beta = 1.5$, it is also shown that the diversity gain is independent to the number of transmit antennas L , as it was analytically proved in Section IV-A.

In Fig. 4, considering BPSK, the SEP is plotted as a function of $\rho = \rho_1 = \rho_2$, for different values of $\bar{\gamma}_{b_t}$. The following parameters were set: $m_1 = 1.5$, $m_3 = 1$, $L = 3$, $\beta = 3$. It is shown that the SEP decreases with the increase of $\bar{\gamma}_{b_t}$ and ρ . It is noted that as ρ increases, i.e., the estimation of the SNR at the selection instance approaches the one at the reception instance, the performance improves. This performance improvement is higher as $\rho \rightarrow 1$. In Fig. 5, considering DBPSK and perfect CSI acquisition, the SEP is plotted as a function of $\bar{\gamma}_{b_t}$, for different values of L . The following parameters were set: $m_1 = 1.5$, $m_3 = 1$, $\beta = 1.5$. It is shown that the SEP decreases with the increase of $\bar{\gamma}_{b_t}$ and L . It is noted that as L increases, the performance improves, with a decreased rate. In the same figure, the asymptotic SEP is also included¹, which approximates, at high SNR, quite well the exact performance. Finally, the diversity order, defined as $DO = -\log(\bar{P}_e) / \log(\text{SNR})$, is also plotted as a function of the SNR for different values of L . As depicted in this figure, as the SNR tends to infinity, the diversity order approaches $d_{L-1} = m_3\beta L$ (with $L \equiv \{2, 3, 4\}$), verifying the analytical results presented in Section IV-A.

In Fig. 6, the normalized channel capacity is plotted as a function of the number of the transmitting antenna L , for different values of ρ as well as for the case of perfect CSI acquisition. The following parameters were set: $m_1 = 1.5$, $m_3 = 1$, $\beta = 3$, $\bar{\gamma}_{b_t} = 10$ dB. In this figure, it is shown that the performance improves with the increase of the number antennas, though with a decreased rate. Moreover, it is also shown that the performance gap (for the different values of ρ) decreases as L decreases, that is the influence of the outdated

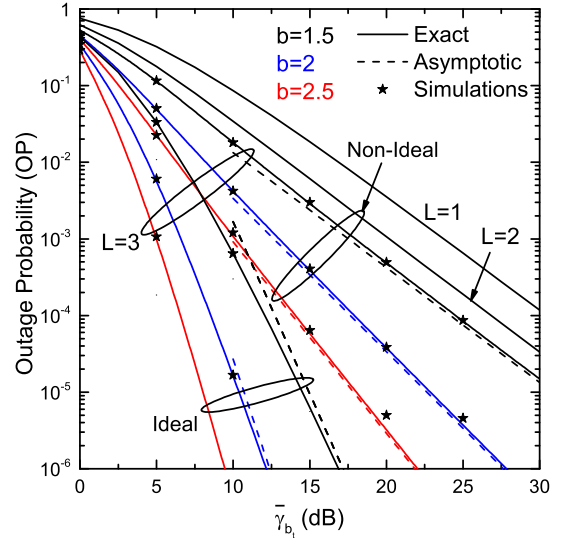


Fig. 3. OP vs $\bar{\gamma}_{b_t}$ for different values of β .

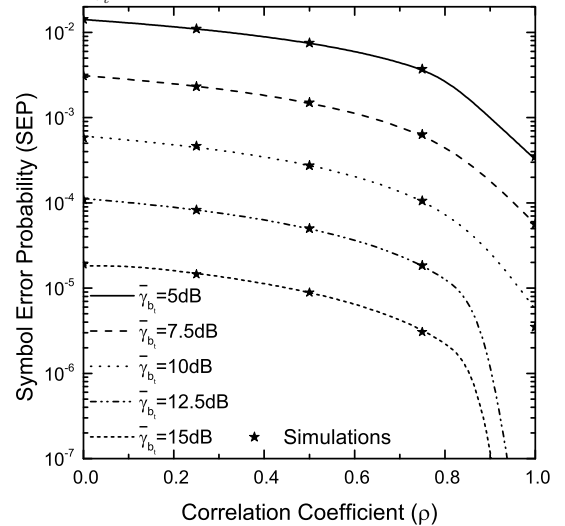


Fig. 4. SEP of BPSK vs ρ for different values of $\bar{\gamma}_{b_t}$.

CSI is higher for higher values of L . Simulation performance results are also included in Figs. 3-6, verifying the validity of the proposed theoretical approach.

In Fig. 7, the normalized LCR, N_R/ω is plotted as a function of the normalized received envelope R_{th}/Ω for different numbers of transmit antennas and under the assumption of perfect and outdated CSI availability. The following parameters were set: $m_1 = 1.5$, $m_3 = 1$, $\beta = 2.1$, $\Omega = 0$ dB. As it is shown in this figure, for lower values of R_{th} , the LCR decreases as L increases, with decreased rate. However, for higher values of R_{th} , i.e., $R_{th} > 0$ dB, the lower rate is obtained when $L = 1$. It should be noted that the performance improvement is significantly lower when outdated CSI is available, whereas the difference between the performance of exact and outdated CSI increases with the increase of L . In Fig. 8, assuming perfect CSI, the normalized AFD is plotted as a function of R_{th} , for different values of L and for the same channel parameters considered in the previous figure. It is shown that for lower values of R_{th} , the TAS

¹The asymptotic expression for the SEP can be directly evaluated using (35) in (38) as $\bar{P}_e \simeq \left(\frac{\Gamma(m_1 - m_3) \bar{\gamma}_1^{m_3}}{b^{-\frac{\beta m_3}{2}} \Gamma(m_1) \Gamma(m_3) m_3} \right)^L a \Gamma \left(1 + \frac{\beta m_3 L}{2} \right)$.

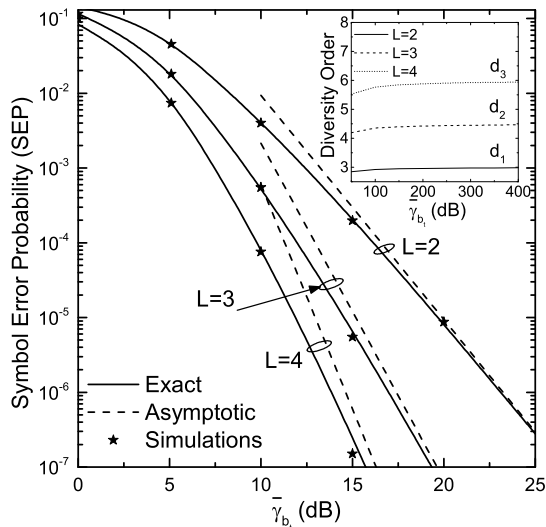


Fig. 5. SEP of DBPSK vs $\bar{\gamma}_{b_t}$ for different values of L .

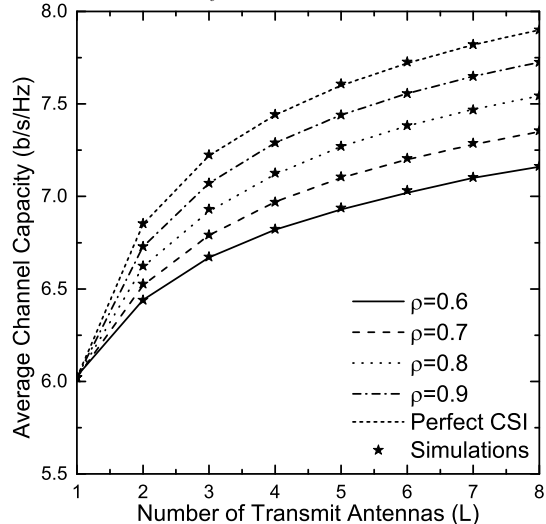


Fig. 6. Normalized channel capacity vs L for different values of ρ and $\bar{\gamma}_{b_t} = 10$ dB.

system spends less time into deep fades. In other words, TAS crosses low values of R_{th} less often than single transmitting systems. Moreover, it is noteworthy that the asymptotic LCR approximates quite close to the exact one, especially for lower values of R_{th} .

VI. CONCLUSIONS

The performance of a TAS scheme operating in a V2V communication environment has been analytically investigated. For the purposes of the analysis, convenient expressions for the bivariate statistics of the dGG distribution have been presented for the first time, including the joint PDF, CDF, and the moments. The dGG fading distribution model is suitably applied for scenarios where double-bouncing mechanism is observed, frequently occurring in M2M communications. In addition, the corresponding marginal expressions were derived, while the second-order statistics of the dGG model were also studied. It was shown that the obtained expressions generalize

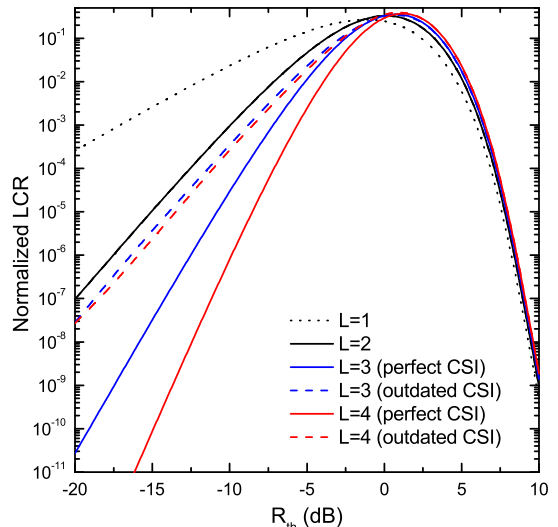


Fig. 7. Normalized LCR vs R_{th} for different values of L .

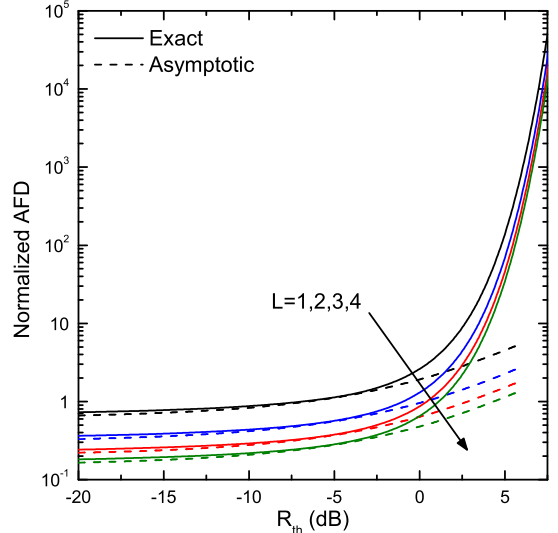


Fig. 8. Normalized AFD vs R_{th} for different values of L .

previously reported results. Based on the derived analysis, the performance of the scheme under consideration has been evaluated using important performance measures, namely OP, SEP, average capacity, the LCR, and the AFD. Finally, the negative consequences of outdated CSI have been analytically demonstrated, using an asymptotic analysis and the derived expressions for the diversity and coding gains.

APPENDIX A PROOF FOR EQUATION (31)

Substituting (28) and (30) in (29), an integral of the following form appears

$$\begin{aligned} \mathcal{I}_1 = & \int_0^\infty x^{\frac{\beta}{2}(p_1+p_3)+\frac{\beta}{2}d_2-1} \exp\left(-2q\sqrt{\hat{\gamma}_1}x^{\frac{\beta}{4}}\right) \\ & \times K_{2p_4+2p_2}\left(2\sqrt{\frac{\hat{\gamma}_2}{\hat{\rho}}}x^{\frac{\beta}{4}}\right) dx. \end{aligned} \quad (\text{A-1})$$

This integral can be solved in closed form by making a change of variables of the form $y = x^{\frac{\beta}{4}}$ and with the aid of [22, Eq. (6.621/3)], yielding at

$$\mathcal{I}_1 = \hat{\gamma}_1^{d_2} D_3, \quad (\text{A-2})$$

in which

$$\begin{aligned} D_3 &= \frac{2^{2d_2-2(q_1+m_1-1)} \sqrt{\pi}}{\beta \hat{\rho}^{p_2+p_4}} \\ &\times \frac{\Gamma(2(m_3+q_2-d_2)) \Gamma(2(m_1+q_1-d_2))}{\left(q + \frac{1}{\sqrt{\hat{\rho}}}\right)^{2(m_3+q_2-d_2)} \Gamma(2(p_1+p_3-d_2))} \\ &\times {}_2F_1 \left[2(m_3+q_2-d_2), 2(p_2+p_4) + \frac{1}{2}; \right. \\ &\quad \left. 2(p_1+p_3-d_2) + \frac{1}{2}; \frac{q - \hat{\rho}^{-1/2}}{q + \hat{\rho}^{-1/2}} \right]. \end{aligned}$$

Based on (A-2), and after some mathematical manipulations, yield the final expression for PDF of output SNR given in (31) and also completes this proof.

APPENDIX B EVALUATION OF INTEGRALS I_A

Assuming ideal feedback, for evaluating the expressions for SEP of BPSK and the capacity, (27) should be substituted in (38) and (44b), respectively, resulting to integrals of the following form

$$\begin{aligned} \mathcal{I}_2 &= \int_0^\infty \gamma^{\frac{\beta}{2}d_2} g(\gamma) \exp\left(-2q\sqrt{\hat{\gamma}_1\gamma^{\frac{\beta}{4}}}\right) d\gamma \\ &\stackrel{(1)}{=} D_4 \left(\frac{b}{2}, \frac{1}{2}\right) \\ &\stackrel{(2)}{=} D_7, \end{aligned} \quad (\text{B-1})$$

in which

$$\begin{aligned} D_4(x, y) &= \frac{\kappa^{1/2} \lambda^{\frac{\beta}{2}d_2+y-\frac{1}{2}}}{x^{\frac{\beta}{2}d_2+y} (2\pi)^{\frac{1}{2}(\lambda+\kappa-2)}} \\ &\times \mathcal{G}_{\lambda, \kappa}^{\kappa, \lambda} \left(\left(\frac{2q\sqrt{\hat{\gamma}_1}}{\kappa} \right)^\kappa \left(\frac{\lambda}{x} \right)^\lambda \middle| \Delta(\lambda, 1-\frac{\beta}{2}d_2-y) \right), \\ D_7 &= \frac{2}{(2\pi)^{\beta+\frac{1}{2}}} \mathcal{G}_{\beta, 4+\beta}^{4+\beta, \beta} \left(\left(\frac{q^2 \hat{\gamma}_1}{4} \right)^2 \middle| \Delta(\beta, -\frac{\beta}{2}d_2) \right), \end{aligned} \quad (\text{B-2})$$

$$(\text{B-3})$$

$\Delta(x, y) = \frac{y}{x}, \frac{y+1}{x}, \dots, \frac{y+x-1}{x}$ and κ, λ are positive integers that satisfy $\lambda/\kappa = \beta/4$. For evaluating the solution (1) in (B-1), $g(\gamma) = \gamma^{y-1} \exp(-x\gamma) = \gamma^{y-1} \mathcal{G}_{0,1}^{1,0} \left(x\gamma \middle| \begin{smallmatrix} - \\ 0 \end{smallmatrix} \right)$ [29, Eq. (11)] is used together with the Meijer G-function representation for the second exponential function, and with the aid of [29, Eq. (21)], yield the closed-form expressions presented in (B-1). As far as (2) is concerned, the same approach is followed with $g(\gamma) = \frac{1}{1+\gamma} = \mathcal{G}_{1,1}^{1,1} \left(\gamma \middle| \begin{smallmatrix} 0 \\ 0 \end{smallmatrix} \right)$ [29, Eq. (10)]. Based on these solutions and after some mathematical manipulations, yield the final expressions for the SEP and the capacity, (39) and (45), respectively, and also completes this proof.

APPENDIX C EVALUATION OF INTEGRALS I_B

Assuming non-ideal feedback, for evaluating the SEP of BPSK and DBPSK, $\text{Aerfc}(\sqrt{B\gamma})$ and $\text{Aexp}(-B\gamma)$, respectively, as well as (31) are substituted in (41), while for the capacity, $\log_2(1+\gamma)$ and (31) are substituted in (44a), resulting to integrals of the following form

$$\begin{aligned} \mathcal{I}_3 &= \int_0^\infty \gamma^{\frac{\beta}{2}(p_1+p_3)-1} g(\gamma) K_{2(p_2+p_4)} \left(\frac{2\sqrt{\hat{\gamma}_1\gamma^{\frac{\beta}{4}}}}{\sqrt{\hat{\rho}}} \right) d\gamma \\ &\stackrel{(1)}{=} D_5 \\ &\stackrel{(2)}{=} D_6 \\ &\stackrel{(3)}{=} D_8, \end{aligned} \quad (\text{C-1})$$

with

$$\begin{aligned} D_5 &= \frac{\left(\frac{\beta}{B}\right)^{\frac{\beta}{2}(p_1+p_3)}}{\sqrt{2}\beta(2\pi)^{\frac{\beta}{2}+1}} \\ &\times \mathcal{G}_{2\beta, 4+\beta}^{4, 2\beta} \left(\left(\frac{\beta}{B} \right)^\beta \hat{\gamma}_1^2 \middle| \begin{array}{c} \Delta(\beta, 1-\frac{\beta}{2}(p_1+p_3)), \Delta(\beta, \frac{1}{2}-\frac{\beta}{2}(p_1+p_3)) \\ \Delta(2, p_2+p_4), \Delta(\beta, -\frac{\beta}{2}(p_1+p_3)) \end{array} \right), \end{aligned} \quad (\text{C-2})$$

$$\begin{aligned} D_6 &= \frac{\left(\frac{\beta}{B}\right)^{\frac{\beta}{2}(p_1+p_3)}}{2\beta^{1/2}(2\pi)^{\frac{1}{2}(\beta+1)}} \\ &\times \mathcal{G}_{\beta, 4}^{4, \beta} \left(\left(\frac{\beta}{B} \right)^\beta \hat{\gamma}_1^2 \middle| \begin{array}{c} \Delta(\beta, 1-\frac{\beta}{2}(p_1+p_3)) \\ \Delta(2, p_2+p_4), \Delta(2, -p_2-p_4) \end{array} \right), \end{aligned} \quad (\text{C-3})$$

$$\begin{aligned} D_8 &= \frac{1}{2\beta \ln(2) (2\pi)^\beta} \mathcal{G}_{2\beta, 4+2\beta}^{4+2\beta, \beta} \left(\left(\frac{\hat{\gamma}_1}{4\hat{\rho}} \right)^2 \middle| \begin{array}{c} \Delta(\beta, -\frac{\beta}{2}(p_1+p_3)), \Delta(\beta, 1-\frac{\beta}{2}(p_1+p_3)) \\ \Delta(2, p_2+p_4), \Delta(2, -(p_2+p_4)), \Delta(\beta, -\frac{\beta}{2}(p_1+p_3)), \Delta(\beta, -\frac{\beta}{2}(p_1+p_3)) \end{array} \right). \end{aligned} \quad (\text{C-4})$$

For evaluating solution (1) in (C-1), $g(\gamma) = \text{erfc}(\sqrt{B\gamma}) = \frac{1}{\sqrt{\pi}} \mathcal{G}_{1,2}^{2,0} \left(B\gamma \middle| \begin{smallmatrix} 1 \\ 0, \frac{1}{2} \end{smallmatrix} \right)$ [35, Eq. (06.27.26.0006.01)] is used together with Meijer G-function representation of the modified Bessel function, i.e., [29, Eq. (14)], and the approach presented in [29, Eq. (21)], yielding the closed-form solutions depicted in (C-1). Moreover, for (2) and (3), the same approach was used with $g(\gamma) = \exp(-B\gamma)$ and $g(\gamma) = \ln(1+\gamma) = \mathcal{G}_{2,2}^{1,2} \left(\gamma \middle| \begin{smallmatrix} 1, 1 \\ 1, 0 \end{smallmatrix} \right)$ [29, Eq. (11)], respectively. Based on these solutions and after some mathematical manipulations, yield the final expressions for the SEPs of BPSK, DBPSK, and the capacity, (42), (43) and (46), respectively, and also completes this proof.

REFERENCES

- [1] P. M. d'Orey and M. Ferreira, "ITS for sustainable mobility: A survey on applications and impact assessment tools," *IEEE Trans. Intell. Transp. Syst.*, vol. 15, no. 2, pp. 477–493, Apr. 2014.
- [2] J. B. Andersen, "Statistical distributions in mobile communications using multiple scattering," in *Proc. 27th URSI General Assembly*, 2002.

- [3] J. Salo, H. M. El-Sallabi, and P. Vainikainen, "Impact of double-Rayleigh fading on system performance," in *Proc. 1st IEEE Int. Symp. on Wireless Pervasive Computing (ISWPC)*, 2006.
- [4] G. K. Karagiannidis, N. C. Sagias, and P. T. Mathiopoulos, "N-Nakagami: A novel stochastic model for cascaded fading channels," *IEEE Trans. Commun.*, vol. 55, no. 8, pp. 1453–1458, Aug. 2007.
- [5] N. C. Sagias and G. S. Tombras, "On the cascaded Weibull fading channel model," *Journal of the Franklin Institute*, vol. 344, no. 1, pp. 1–11, 2007.
- [6] E. Vinogradov, W. Joseph, and C. Oestges, "Measurement-based modeling of time-variant fading statistics in indoor peer-to-peer scenarios," *IEEE Trans. Antennas Propag.*, vol. 63, no. 5, pp. 2252–2263, May 2015.
- [7] N. Zlatanov, Z. Hadzi-Velkov, and G. K. Karagiannidis, "Level crossing rate and average fade duration of the double Nakagami-m random process and application in MIMO keyhole fading channels," *IEEE Commun. Lett.*, vol. 12, no. 11, pp. 822–824, Nov. 2008.
- [8] R. Khedhiri, N. Hajri, N. Youssef, and M. Patzold, "On the first- and second-order statistics of selective combining over double Nakagami-m fading channels," in *Proc. IEEE 80th Vehicular Technology Conference (VTC-Fall)*, Sep. 2014.
- [9] M. L. Ammari and S. Roy, "Performance analysis of diversity combining techniques in double-Rayleigh channels," in *Proc. International Conference on Computing, Networking and Communications (ICNC)*, Feb. 2016, pp. 1–6.
- [10] L. Xu, H. Zhang, J. Wang, and T. A. Gulliver, "Performance analysis of the double-antenna SDC system over N-Nakagami fading channels," *International Journal of Wireless Information Networks*, vol. 23, no. 1, pp. 49–56, 2016.
- [11] H. AlQuwaiee, I. S. Ansari, and M. S. Alouini, "On the performance of free-space optical communication systems over double generalized gamma channel," *IEEE J. Sel. Areas Commun.*, vol. 33, no. 9, pp. 1829–1840, Sep. 2015.
- [12] —, "On the maximum and minimum of double generalized gamma variates with applications to the performance of free-space optical communication systems," *IEEE Trans. Veh. Technol.*, vol. 65, no. 11, pp. 8822–8831, Nov. 2016.
- [13] Y. Chen, G. K. Karagiannidis, H. Lu, and N. Cao, "Novel approximations to the statistics of products of independent random variables and their applications in wireless communications," *IEEE Trans. Veh. Technol.*, vol. 61, no. 2, pp. 443–454, Feb. 2012.
- [14] E. F. Abd-Elfattah, "Saddlepoint density and distribution functions for the ratio of two linear functions and the product of generalized gamma variates," *Communications in Statistics - Theory and Methods*, 2017.
- [15] A. Yilmaz, F. Yilmaz, M. S. Alouini, and O. Kucur, "On the performance of transmit antenna selection based on shadowing side information," *IEEE Trans. Veh. Technol.*, vol. 62, no. 1, pp. 454–460, Jan. 2013.
- [16] L. Xu, J. Wang, H. Zhang, and T. A. Gulliver, "Performance analysis of IAF relaying mobile D2D cooperative networks," *Journal of the Franklin Institute*, vol. 354, no. 2, pp. 902–916, 2017.
- [17] Y. Alghorani and M. Seyfi, "On the performance of reduced-complexity transmit/receive-diversity systems over MIMO-V2V channel model," *IEEE Wireless Commun. Lett.*, vol. 6, no. 2, pp. 214–217, April 2017.
- [18] S. O. Ata and I. Altunbas, "Joint relay and antenna selection in MIMO PLNC inter-vehicular communication systems over cascaded fading channels," *Wireless Pers. Commun.*, vol. 92, no. 3, pp. 901–923, 2017.
- [19] X. Lei, W. Zhou, P. Fan, and L. Fan, "Impact of outdated channel state information on multiuser cooperative relay networks in co-channel interference environments," in *Proc. IEEE International Conference on Communications in China (ICCC)*, 2012, pp. 503–507.
- [20] P. S. Bithas, K. Maliatsos, and A. G. Kanatas, "The bivariate double Rayleigh distribution for multichannel time-varying systems," *IEEE Wireless Commun. Lett.*, vol. 5, no. 5, pp. 524–527, Oct. 2016.
- [21] M. D. Yacoub, "The α - μ distribution: A physical fading model for the Stacy distribution," *IEEE Trans. Veh. Technol.*, vol. 56, no. 1, pp. 27–34, Jan. 2007.
- [22] I. S. Gradshteyn and I. M. Ryzhik, *Table of Integrals, Series, and Products*, 6th ed. New York: Academic Press, 2000.
- [23] A. Coulson, A. Williamson, and R. Vaughan, "Improved fading distribution for mobile radio," *IEE Proceedings-Communications*, vol. 145, no. 3, pp. 197–202, 1998.
- [24] M. Abramowitz and I. A. Stegun, *Handbook of mathematical functions: with formulas, graphs, and mathematical tables*. Courier Corporation, 1964, vol. 55.
- [25] F. Gong, J. Ge, and N. Zhang, "SER analysis of the mobile-relay-based M2M communication over double Nakagami-m fading channels," *IEEE Commun. Lett.*, vol. 15, no. 1, pp. 34–36, Jan. 2011.
- [26] P. S. Bithas, A. G. Kanatas, D. B. da Costa, and P. K. Upadhyay, "Transmit antenna selection in vehicle-to-vehicle time-varying fading channels," in *Proc. IEEE International Conference on Communications (ICC)*, May 2017.
- [27] A. Papoulis, *Probability, Random Variables, and Stochastic Processes*, 2nd ed. New York: McGraw-Hill, 1984.
- [28] M. Simon, *Probability Distributions Involving Gaussian Random Variables*, 1st ed. Springer, 2006.
- [29] V. S. Adamchik and O. I. Marichev, "The algorithm for calculating integrals of hypergeometric type functions and its realization in REDUCE system," in *Proc. International Conference on Symbolic and Algebraic Computation*, Tokyo, Japan, 1990, pp. 212–224.
- [30] A. Krantzik and D. Wolf, "Distribution of the fading intervals of modified Suzuki process," in *Signal Processing V: Theories and Applications*, L. Torres, E. Masgrau, and M. A. Lagunas, Eds. Amsterdam, The Netherlands: Elsevier Sciences, pp. 361–364, Jan. 1990.
- [31] C. D. Iskander and P. T. Mathiopoulos, "Analytical level crossing rates and average fade durations for diversity techniques in Nakagami fading channels," *IEEE Trans. Commun.*, vol. 50, no. 8, pp. 1301–1309, Aug. 2002.
- [32] S. Khalili et al., "Code-aided channel tracking and decoding over sparse fast-fading multipath channels with an application to train backbone networks," *IEEE Trans. Intell. Transp. Syst.*, vol. 18, no. 3, pp. 481–492, Mar. 2017.
- [33] Y. Gu, S. Ikki, and S. Aissa, "Opportunistic cooperative communication in the presence of co-channel interferences and outdated channel information," *IEEE Commun. Lett.*, vol. 17, no. 10, pp. 1948–1951, Oct. 2013.
- [34] A. Prudnikov, Y. Brychkov, and O. Marichev, *Integrals and Series, Volume 2*. Gordon and Breach Science Publishers, 1986.
- [35] The Wolfram Functions Site, 2017. [Online]. Available: <http://functions.wolfram.com>
- [36] Y. Chen and C. Tellambura, "Distribution functions of selection combiner output in equally correlated Rayleigh, rician, and Nakagami-m fading channels," *IEEE Trans. Commun.*, vol. 52, no. 11, pp. 1948–1956, Nov. 2004.
- [37] A. Prudnikov, Y. Brychkov, and O. Marichev, *Integrals and Series, Volume 1*. Gordon and Breach Science Publishers, 1986.
- [38] M. Al-Abadi and A. Dutta, "Predictive analytics for non-stationary V2I channel," in *Proc. 9th International Conference on Communication Systems and Networks (COMSNETS)*, Jan. 2017, pp. 243–250.
- [39] N. Lee and R. W. Heath, "Space-time interference alignment and degree-of-freedom regions for the MISO broadcast channel with periodic CSI feedback," *IEEE Trans. Inf. Theory*, vol. 60, no. 1, pp. 515–528, 2014.



Petros S. Bithas (S'04-M'09) received the B.S. in electrical engineering from the Department of Electrical and Computer Engineering of the University of Patras, Greece, in 2003. From the same Department he received the Ph.D. degree with specialization in "Wireless Communication Systems" in 2009. During 2004–2009, he was a research assistant at the Institute for Space Applications and Remote Sensing (ISARS) of the National Observatory of Athens (NOA), Greece. Since October 2009 he is affiliated with the Department of electronics engineering of the Technological Educational Institute of Piraeus as a Lab Instructor. Furthermore, during the November of 2010 and February 2013 he was a postdoctoral researcher at the Department of Digital Systems, University of Piraeus and during the April 2013 and September 2015 he was affiliated with the Institute for Astronomy, Astrophysics, Space Applications and Remote Sensing (IAASARS) of the NOA. Since May 2015 he is a postdoctoral researcher at the Department of Digital Systems, University of Piraeus.

Dr Bithas serves on the Editorial Board of the International Journal of Electronics and Communications (ELSEVIER). He has been selected as an "Exemplary Reviewer" of the IEEE COMMUNICATIONS LETTERS for year 2010, while he is also co-recipient of Best Paper Awards at the IEEE International Symposium on Signal Processing and Information Technology, 2013. He has published 28 articles in international scientific journals and 32 articles in the proceedings of international conferences. His current research interests include stochastic modeling of wireless communication channels as well as design and performance analysis of V2V communication systems.



Athanasios (Thanasis) G. Kanatas (S'90-M'93-SM'02) is a Professor at the Department of Digital Systems and Dean of the School of Information & Communication Technologies at the University of Piraeus, Greece. He received the Diploma in Electrical Engineering from the National Technical University of Athens (NTUA), Greece, in 1991, the M.Sc. degree in Satellite Communication Engineering from the University of Surrey, Surrey, UK in 1992, and the Ph.D. degree in Mobile Satellite Communications from NTUA, Greece in February 1997. From 1993

to 1994, he was with National Documentation Center of National Research Institute. In 1995, he joined SPACETEC Ltd. as Technical Project Manager for VISA/EMEA VSAT Project in Greece. In 1996, he joined the Mobile Radio-Communications Laboratory as a research associate. From 1999 to 2002 he was with the Institute of Communication & Computer Systems responsible for the technical management of various research projects. In 2000, he became a member of the Board of Directors of OTESAT S.A. In 2002, he joined the University of Piraeus as an Assistant Professor. He has published more than 150 papers in International Journals and International Conference Proceedings. He is the author of 6 books in the field of wireless and satellite communications in Greek and/or English language. He has been the technical manager of several European and National R&D projects. His current research interests include the development of new digital techniques for wireless and satellite communications systems, channel characterization, simulation, and modeling for mobile, mobile satellite, and future wireless communication systems, antenna selection and RF preprocessing techniques, new transmission schemes for MIMO systems, V2V communications, and energy efficient techniques for Wireless Sensor Networks. He has been a Senior Member of IEEE since 2002. In 1999, he was elected Chairman of the Communications Society of the Greek Section of IEEE.



Daniel Benevides da Costa (S'04-M'08-SM'14) was born in Fortaleza, Ceará, Brazil, in 1981. He received the B.Sc. degree in Telecommunications from the Military Institute of Engineering (IME), Rio de Janeiro, Brazil, in 2003, and the M.Sc. and Ph.D. degrees in Electrical Engineering, Area: Telecommunications, from the University of Campinas, SP, Brazil, in 2006 and 2008, respectively. His Ph.D. thesis was awarded the Best Ph.D. Thesis in Electrical Engineering by the Brazilian Ministry of Education (CAPES) at the 2009 CAPES Thesis Contest. From

2008 to 2009, he was a Postdoctoral Research Fellow with INRS-EMT, University of Quebec, Montreal, QC, Canada. Since 2010, he has been with the Federal University of Ceará, where he is currently an Assistant Professor. Prof. da Costa is currently Editor of the IEEE COMMUNICATIONS SURVEYS AND TUTORIALS, IEEE ACCESS, IEEE TRANSACTIONS ON COMMUNICATIONS, IEEE TRANSACTIONS ON VEHICULAR TECHNOLOGY, EURASIP JOURNAL ON WIRELESS COMMUNICATIONS AND NETWORKING, and KSII TRANSACTIONS ON INTERNET AND INFORMATION SYSTEMS. He has also served as Associate Technical Editor of the IEEE COMMUNICATIONS MAGAZINE. From 2012 to 2017, he was Editor of the IEEE COMMUNICATIONS LETTERS. He has served as Guest Editor of several Journal Special Issues. He has been involved on the Organizing Committee of several conferences. He is currently the Latin American Chapters Coordinator of the IEEE Vehicular Technology Society. Also, he acts as a Scientific Consultant of the National Council of Scientific and Technological Development (CNPq), Brazil and he is a Productivity Research Fellow of CNPq. From 2012 to 2017, he was Member of the Advisory Board of the Cear Council of Scientific and Technological Development (FUNCAP), Area: Telecommunications. Prof. da Costa is the recipient of three conference paper awards. He received the Exemplary Reviewer Certificate of the IEEE WIRELESS COMMUNICATIONS LETTERS in 2013, the Exemplary Reviewer Certificate of the IEEE COMMUNICATIONS LETTERS in 2016, the Certificate of Appreciation of Top Associate Editor for outstanding contributions to IEEE TRANSACTIONS ON VEHICULAR TECHNOLOGY in 2013, 2015 and 2016, and the Exemplary Editor Award of IEEE COMMUNICATIONS LETTERS in 2016. He is a Distinguished Lecturer of the IEEE Vehicular Technology Society. He is a Senior Member of IEEE, Member of IEEE Communications Society and IEEE Vehicular Technology Society.



Prabhat K. Upadhyay (S'09-M'13-SM'16) received the Ph.D. degree in Electrical Engineering from Indian Institute of Technology (IIT) Delhi, New Delhi, India, in 2011. Previously, he was a Lecturer with the Department of Electronics and Communication Engineering, Birla Institute of Technology (BIT) Mesra, Ranchi. Since 2012, he has been an Assistant Professor with the Discipline of Electrical Engineering, IIT Indore, where he has also been leading various research projects in Wireless Communications (WiCom) Research Group. He has

numerous publications in peer-reviewed journals and conferences, and has authored a book and a book chapter. His main research interests include wireless relaying techniques, cooperative communications, multiple-input-multiple-output signal processing, hybrid satellite-terrestrial systems, cognitive radio, physical layer security, and molecular communications. He has been selected for Sir Visvesvaraya Young Faculty Research Fellowship under Ministry of Electronics and Information Technology, Government of India. He is a Senior Member of the IEEE, Member of the IEEE Communications Society and IEEE Vehicular Technology Society, and Life Member of the Institution of Electronics and Telecommunication Engineers.



Ugo Silva Dias (S'04-M'08) was born in Belém, Pará, Brazil, in 1981. He received the B.Sc. degree in Electrical Engineering from the Federal University of Pará, Brazil, in 2004, and the M.Sc. and Ph.D. degrees in Electrical Engineering, Area: Telecommunications, from the University of Campinas, Brazil, in 2006 and 2010, respectively. Since March 2010, Dr. Ugo Dias is Professor at University of Brasilia (UnB), Brazil. He is a faculty member of the Department of Electrical Engineering, MWSL Lab and Latitude Lab. His main research interests include

fading channels, field measurements, coexistence of future networks, cognitive radio, and wireless technologies in general. Prof. Dias is currently Editor of the IET ELECTRONICS LETTERS and ACTA PRESS - COMMUNICATIONS. He has been involved on the Organizing Committee of several conferences. He is the recipient of two conference paper awards. Besides the academic experiences, he also worked in several companies in the ICT industry. Prof. Dias is currently chair of the IEEE ComSoc CN Brazil Chapter, IT director of the Brazilian Telecommunications Society, and Advisor of Brazilian Internet Steering Committee. He is a Member of IEEE, IEEE Communications Society, Brazilian Telecommunications Society, and Brazilian Communications Committee.